

## Formation of Oxide Phases in the System Pr-Fe-O

Mira Ristić,<sup>a,\*</sup> Stanko Popović,<sup>b</sup> and Svetozar Musić<sup>a</sup>

<sup>a</sup>Ruđer Bošković Institute, Bijenička cesta 54, P. O. Box 180, Zagreb, HR-10002, Croatia

<sup>b</sup>Department of Physics, Faculty of Science, University of Zagreb, Zagreb, HR-10000, Croatia

RECEIVED MARCH 8, 2013; REVISED JULY 22, 2013; ACCEPTED SEPTEMBER 2, 2013

**Abstract.** The formation of oxide phases at 900 °C in the system Fe<sub>2</sub>O<sub>3</sub>-“Pr<sub>2</sub>O<sub>3</sub>” was investigated. With a decrease in the molar fraction of Fe<sub>2</sub>O<sub>3</sub> a corresponding increase in PrFeO<sub>3</sub> was observed. For equal molar fractions of Fe<sub>2</sub>O<sub>3</sub> and “Pr<sub>2</sub>O<sub>3</sub>” the formation of PrFeO<sub>3</sub> and very small fractions of α-Fe<sub>2</sub>O<sub>3</sub> plus an additional oxide phase, which could not be identified with certainty, were observed. With further increase in “Pr<sub>2</sub>O<sub>3</sub>” fraction the praseodymium oxides Pr<sub>6</sub>O<sub>11</sub> and PrO<sub>2</sub> started to become dominant in the phase composition. The small fraction (< 0.02) of the same unidentified oxide phase was also obtained when Pr(OH)<sub>3</sub> was calcined in air at 900 °C; this was probably a mixture of other praseodymium oxides with different average oxidation numbers of Pr. The results of XRD, <sup>57</sup>Fe Mössbauer and FT-IR spectroscopies are discussed. (doi: [10.5562/cca2247](https://doi.org/10.5562/cca2247))

**Keywords:** α-Fe<sub>2</sub>O<sub>3</sub>, PrFeO<sub>3</sub>, praseodymium oxides

### INTRODUCTION

RE-orthoferrites (RE = rare earth) and their substituted compounds are in the focus of many studies due to their specific magnetic, electrical and chemical properties. These materials have potential applications in solid-state fuel cells, catalysis or as various types of sensors. The microstructural properties of RE-orthoferrites can be changed by the synthesis route or substitution of Fe with selected metal cations.

Rajendran *et al.*<sup>1</sup> prepared thin films of selected RE-orthoferrites on fused silica using sol-gel processing combined with calcination at 650 °C. Sivakumar *et al.*<sup>2</sup> prepared nanocrystalline orthoferrites GdFeO<sub>3</sub>, ErFeO<sub>3</sub>, TbFeO<sub>3</sub> and EuFeO<sub>3</sub> starting from Fe(CO)<sub>5</sub> and corresponding RE-carbonate with the aid of sonochemistry. The orthoferrite precursors were then calcined between 800 and 910 °C for 24 h in air atmosphere. Rajendran and Bhattacharya<sup>3</sup> reported the formation of nanocrystalline orthoferrite powders of selected RE cations combining the coprecipitation and calcination of the gel precursor at 650 to 700 °C in air. The coprecipitation method was also used<sup>4</sup> to prepare DyFeO<sub>3</sub>. To a solution of DyCl<sub>3</sub> and FeCl<sub>2</sub> salts NaOH solution was added, the coprecipitate was washed and dried, then heated in air at 700 to 1000 °C. In this temperature range XRD showed

the formation of a DyFeO<sub>3</sub> phase. RE-orthoferrites of La, Pr and Nd were synthesized at 400 °C using a molten NaOH flux.<sup>5</sup> Li *et al.*<sup>6</sup> prepared RE orthoferrites (RE = La, Pr-Tb) in the form of hollow spheres or solid spheres (RE = Dy-Yb, Y) using the calcination of the RE-Fe citrate complex at ~ 800 °C. All these RE-orthoferrites were successfully used for catalytical reduction of NO pollutant by CO at 200 to 500 °C and their efficiency could be compared with noble metal catalysts. The effect of Ca<sup>2+</sup> substitution on the structural and magnetic properties of RE-orthoferrite was investigated.<sup>7</sup> Also, (RE)<sub>0.7</sub>Ca<sub>0.3</sub>FeO<sub>3</sub>, RE = La, Dy, Y, Er or Gd were investigated for possible applications as pressure or γ-ray sensor.<sup>8</sup> The structural, morphological and transport properties influenced by doping Ni for Fe in PrFeO<sub>3</sub> ceramic thin films were investigated as well.<sup>9</sup> Saraswat *et al.*<sup>10</sup> prepared the hydroxide coprecipitate Fe(OH)<sub>3</sub>/Pr(OH)<sub>3</sub> containing Fe(III) (*w* = 5 %). The coprecipitate was heated up to 1100 °C. In the present work we extended the investigation of the system Fe<sub>2</sub>O<sub>3</sub>-“Pr<sub>2</sub>O<sub>3</sub>” by varying the molar fractions of Fe<sub>2</sub>O<sub>3</sub> and “Pr<sub>2</sub>O<sub>3</sub>” with the aim to identify the actual crystal phases formed in this mixed oxides system. Praseodymium has a much more complex oxide chemistry than the other rare earths and this is probably one of the reasons why the formation of PrFeO<sub>3</sub> has been less investigated.

\* Author to whom correspondence should be addressed. (E-mail: [ristic@irb.hr](mailto:ristic@irb.hr))

**Table 1.** XRD analysis of the samples prepared in the system  $\text{Fe}_2\text{O}_3$ -“ $\text{Pr}_2\text{O}_3$ ” where “ $\text{Pr}_2\text{O}_3$ ” is virtual composition and X is unknown phase

Sample	Initial (molar) ratio $\text{Fe}_2\text{O}_3$ -“ $\text{Pr}_2\text{O}_3$ ”	Phase composition as found by XRD (approx. molar fraction in brackets)
S1	99 : 1	$\alpha$ - $\text{Fe}_2\text{O}_3$ + $\text{PrFeO}_3$ (0.02)
S2	97 : 3	$\alpha$ - $\text{Fe}_2\text{O}_3$ + $\text{PrFeO}_3$ (0.06)
S3	95 : 5	$\alpha$ - $\text{Fe}_2\text{O}_3$ + $\text{PrFeO}_3$ (0.1)
S4	90 : 10	$\alpha$ - $\text{Fe}_2\text{O}_3$ + $\text{PrFeO}_3$ (0.2)
S5	85 : 15	$\alpha$ - $\text{Fe}_2\text{O}_3$ + $\text{PrFeO}_3$ (0.3)
S6	80 : 20	$\alpha$ - $\text{Fe}_2\text{O}_3$ + $\text{PrFeO}_3$ (0.4)
S7	70 : 30	$\text{PrFeO}_3$ + $\alpha$ - $\text{Fe}_2\text{O}_3$ (0.4)
S8	50 : 50	$\text{PrFeO}_3$ + $\alpha$ - $\text{Fe}_2\text{O}_3$ (~0.01) + X (< 0.02)
S9	30 : 70	$\text{Pr}_6\text{O}_{11}$ ( $\leq 1/2$ ) + $\text{PrFeO}_3$ ( $\leq 1/2$ ) + $\text{PrO}_2$ (0.05) + X (< 0.02)
S10	10 : 90	$\text{Pr}_6\text{O}_{11}$ + $\text{PrO}_2$ (0.20) + $\text{PrFeO}_3$ (0.10) + X (< 0.02)
S11	“ $\text{Pr}_2\text{O}_3$ ”	$\text{Pr}_6\text{O}_{11}$ <sup>(a)</sup> + $\text{PrO}_2$ <sup>(b)</sup> + X (< 0.02)

<sup>(a)</sup> Identified according JCPDS PDF card No. 6-329<sup>(b)</sup> Identified according JCPDS PDF card No. 24-1006

## EXPERIMENTAL

Analytical grade chemicals,  $\text{Fe}(\text{NO}_3)_3 \cdot 9 \text{H}_2\text{O}$ ,  $\text{Pr}(\text{NO}_3)_3 \cdot 6 \text{H}_2\text{O}$  and 25 %  $\text{NH}_3(\text{aq})$ , were used. Twice-distilled water was prepared in own laboratory. Mixed hydroxides  $\text{Fe}(\text{OH})_3/\text{Pr}(\text{OH})_3$  were quantitatively coprecipitated by adding  $\text{NH}_4\text{OH}$  solution to an aqueous solution of  $\text{Fe}(\text{NO}_3)_3$  +  $\text{Pr}(\text{NO}_3)_3$  salts. The hydroxide coprecipitates were washed by centrifugation without permitting the peptization of the mixed hydroxide coprecipitate. After drying the coprecipitates were heated in air at 200 °C for 1 h, 400 °C for 1 h, 500 °C for 1 h, 600 °C for 1 h and 900 °C for 4 h. When the heating time was over, the crucibles were removed from the oven and cooled in air to room temperature (RT).

XRD patterns were recorded at RT using the Philips MPD 1880 diffractometer (Cu-K $\alpha$  radiation, graphite monochromator and proportional counter).  $^{57}\text{Fe}$  Mössbauer spectra were recorded at 20 °C in the transmission mode using the spectrometer setup with WissEl (Starnberg, Germany) products.  $^{57}\text{Co}$  in Rh matrix was used as Mössbauer source. The velocity scale and Mössbauer parameters refer to the metallic  $\alpha$ -Fe absorber at 20 °C. The raw spectra were fitted using the MossWin program.

FT-IR spectra were recorded at RT with Perkin-Elmer spectrometer (model 2000). Powders were mixed with spectroscopically pure KBr and pressed into tablets using a Carver press. The particles were inspected with a JEOL thermal field emission scanning electron microscope (model JSM-7000F). The inspected particles were not coated with an electrically conductive layer.

## RESULTS AND DISCUSSION

The results of XRD phase analysis of samples S1 to S11 with different initial molar ratios in the system  $\text{Fe}_2\text{O}_3$ -“ $\text{Pr}_2\text{O}_3$ ” are given in Table 1. The oxides of  $\alpha$ - $\text{Fe}_2\text{O}_3$  and  $\text{PrFeO}_3$  phases were found in the samples prepared in the initial molar ratio  $\alpha$ - $\text{Fe}_2\text{O}_3$ :“ $\text{Pr}_2\text{O}_3$ ” = 70:30 (samples S1 to S7). The phase analysis of sample S8 prepared from equal initial molar ratios of  $\text{Fe}_2\text{O}_3$  and “ $\text{Pr}_2\text{O}_3$ ” showed the formation of  $\text{PrFeO}_3$  and a very small fraction of  $\alpha$ - $\text{Fe}_2\text{O}_3$  (~0.01) plus an undetermined phase X (< 0.02). With an increase in the heating temperature up to 1100 °C the orthoferrite  $\text{PrFeO}_3$ , as a single phase, is formed. With further increase in the starting “ $\text{Pr}_2\text{O}_3$ ” fraction there is a corresponding decrease in the  $\text{PrFeO}_3$  fraction accompanied by the appearance of praseodymium oxide phases,  $\text{Pr}_6\text{O}_{11}$  and  $\text{PrO}_2$ . The  $\text{Pr}_6\text{O}_{11}$ ,  $\text{PrO}_2$  and X (< 0.02) phases were obtained when only the  $\text{Pr}(\text{OH})_3$  precursor was used (sample S11). The fraction X (< 0.02) was not identified with certainty due to very small intensities of diffraction lines and possible overlapping of several other praseodymium oxides. Apart from  $\text{Pr}_2\text{O}_3$  with oxidation number  $\text{Pr}^{3+}$  and  $\text{PrO}_2$  with oxidation number  $\text{Pr}^{4+}$  there were several other praseodymium oxides with varying average oxidation numbers such as  $\text{Pr}_7\text{O}_{12}$ ,  $\text{Pr}_9\text{O}_{16}$ ,  $\text{Pr}_5\text{O}_9$ ,  $\text{Pr}_{11}\text{O}_{20}$  and  $\text{Pr}_6\text{O}_{11}$ .<sup>11</sup> The formation of these oxide phases depends on the maximum heating temperature, annealing and the cooling atmosphere. In this respect the oxide chemistry of praseodymium is specific among other rare earth elements. More about the stoichiometry of praseodymium oxides is reported in selected references.<sup>12-15</sup>

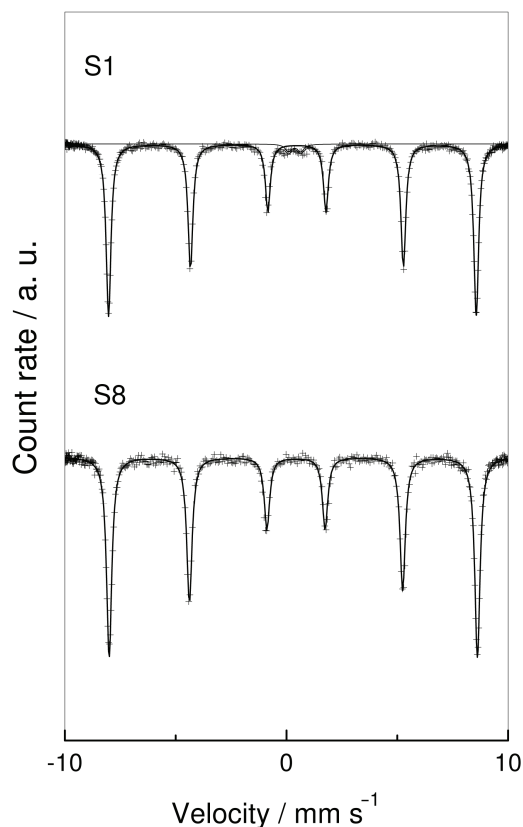


**Figure 1.**  $^{57}\text{Fe}$  Mössbauer spectra of samples S1 and S8, recorded at 20 °C.

Figure 1. shows the Mössbauer spectra of the selected samples (S1 and S8), whereas the calculated Mössbauer parameters for all Fe-containing samples are given in Table 2. RT Mössbauer spectra of  $\alpha\text{-Fe}_2\text{O}_3$  and  $\text{PrFeO}_3$  showed magnetic hyperfine structure (MHS) with similar Mössbauer parameters. For that reason these two hyperfine magnetically splitted subspectra were fitted as one sextet. The presence of the  $\text{PrFeO}_3$  phase in dependence on a decrease in the  $\alpha\text{-Fe}_2\text{O}_3$  fraction can be monitored only on the basis of changes in quadrupole splitting, as clearly discernible in Table 2.

The Mössbauer spectrum of sample S1 showed the superposition of one sextet (M) and one central quadrupole doublet (Q) of small relative intensity. The parameters of sextet M corresponds to  $\alpha\text{-Fe}_2\text{O}_3$  phase.<sup>16</sup> Taking into account the results of XRD measurement the central quadrupole doublet Q can be assigned to very fine  $\text{PrFeO}_3$  crystallites. The dissolution of  $\text{Pr}^{3+}$  cation into  $\alpha\text{-Fe}_2\text{O}_3$  crystal structure is not likely, due to a great difference in the ionic radii of  $\text{Fe}^{3+}$  and  $\text{Pr}^{3+}$  cations. Samples S2 to S8 show only one sextet which is actually a superposition of two sextets with similar parameters. Eibschütz *et al.*<sup>17</sup> measured the Mössbauer spectra of different RE-orthoferrites including  $\text{PrFeO}_3$ . At 296 K, the following parameters for  $\text{PrFeO}_3$  were measured: HMF = 51.0 T and Eq = 0.012

**Table 2.** Calculated Mössbauer parameters at 20 °C, where  $\delta$  is isomer shift;  $\Delta$  or Eq is quadrupole splitting; HMF is hyperfine magnetic field. Isomer shift,  $\delta$ , is given relative to  $\alpha\text{-Fe}$  at 20 °C.

Sample	Line	$\delta^{(a)}$ / $\text{mm s}^{-1}$	$\Delta$ or Eq <sup>(b)</sup> / $\text{mm s}^{-1}$	HMF <sup>(c)</sup> / T	$\Gamma$ / $\text{mm s}^{-1}$	Area/ %
S1	M	0.37	-0.20	51.5	0.26	97.4
	Q	0.37	0.55	–	0.35	2.6
S2	M	0.37	-0.20	51.5	0.27	100
S3	M	0.37	-0.19	51.5	0.27	100
S4	M	0.37	-0.19	51.5	0.27	100
S5	M	0.37	-0.17	51.5	0.28	100
S6	M	0.37	-0.17	51.5	0.28	100
S7	M	0.37	-0.14	51.4	0.27	100
S8	M	0.37	-0.12	51.4	0.27	100
S9	M	0.37	-0.04	51.2	0.27	100
S10	M	0.37	-0.02	51.2	0.27	100

<sup>(a)</sup> Error  $\delta = \pm 0.01 \text{ mm s}^{-1}$

<sup>(b)</sup> Error  $\Delta$  or Eq =  $\pm 0.01 \text{ mm s}^{-1}$

<sup>(c)</sup> Error HMF =  $\pm 0.2 \text{ T}$

$\text{mm s}^{-1}$ . Saraswat *et al.*<sup>10</sup> measured RT Mössbauer parameters for  $\text{PrFeO}_3$ : HMF = 50.6 T and Eq = 0.06  $\text{mm s}^{-1}$ . A difference in Mössbauer parameters for  $\text{PrFeO}_3$  can be assigned to different ways of the formation of this orthoferrite. Pasternak *et al.*<sup>18</sup> investigated the high-pressure (HP) structural, magnetic and electronic properties of RE-orthoferrites with the large ( $\text{La}^{3+}$ ,  $\text{Pr}^{3+}$ ), the intermediate ( $\text{Eu}^{3+}$ ,  $\text{Y}^{3+}$ ) or the smallest  $\text{Lu}^{3+}$  cations.  $\text{PrFeO}_3$  subjected to high pressure shows two equally abundant magnetic sublattices due to high-spin and low-spin  $\text{Fe}^{3+}$  sites. Starting with 40 GPa the RT Mössbauer spectra show a superposition of two central quadrupole doublets. The quadrupole doublet with smaller  $\Delta$  and  $\delta$  corresponds to the HS sublattice. By cooling  $\text{PrFeO}_3$  to 5 K both high-spin (HS) and low-spin (LS) subspectra become magnetically ordered.<sup>18</sup>

FT-IR spectra of samples S1 to S10 also show gradual changes in dependence on the initial molar ratio  $\text{Fe}_2\text{O}_3$ : “ $\text{Pr}_2\text{O}_3$ ”. The spectrum of sample S1, shown in Figure 2., can be assigned to the hematite phase. Hematite ( $D_{3d}^6$  symmetry) is characterized by six IR active vibrations, two  $A_{2u}$  ( $E||C$ ) and four  $E_u$  ( $E \perp C$ ).<sup>19,20</sup> In the present case, for sample S1 these vibrations were recorded at 630  $\text{cm}^{-1}$  ( $A_{2u}$ ), 550  $\text{cm}^{-1}$  ( $E_u$ ), 475  $\text{cm}^{-1}$  ( $E_u$ ), 390  $\text{cm}^{-1}$  ( $A_{2u}$ ) and 344  $\text{cm}^{-1}$  ( $E_u$ ). Different factors, such as crystallinity, size and morphology of hematite particles determine the positions of the corresponding IR bands. With an increase in “ $\text{Pr}_2\text{O}_3$ ” molar fraction the IR band at 630  $\text{cm}^{-1}$ , as well as IR band at 390  $\text{cm}^{-1}$  are diminishing. The FT-IR spectrum of sample S8 with  $\text{PrFeO}_3$  molar fraction larger than 0.97, as found with XRD, shows

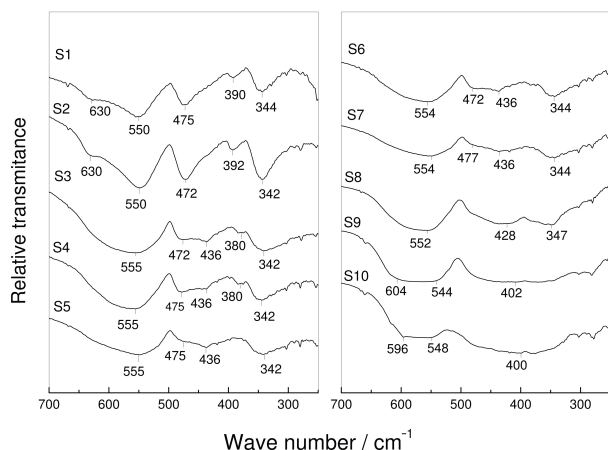


**Figure 2.** FT-IR spectra of samples S1 to S10, recorded at RT.

three IR bands positioned at 552, 428 and 347  $\text{cm}^{-1}$ . Two strong IR bands at  $\sim 560 \text{ cm}^{-1}$  and  $\sim 440 \text{ cm}^{-1}$  were recorded for  $\text{EuFeO}_3$ ,  $\text{GdFeO}_3$ ,  $\text{TbFeO}_3$  and  $\text{ErFeO}_3$ .<sup>2</sup> The IR band at  $\sim 560 \text{ cm}^{-1}$  was assigned to the Fe–O stretching vibration, whereas the  $\sim 440 \text{ cm}^{-1}$  band was interpreted as O–Fe–O deformation vibration. Sivakumara<sup>5</sup> recorded the IR bands at 562, 421 and 381  $\text{cm}^{-1}$  for  $\text{PrFeO}_3$ , similar to the case of  $\text{LaFeO}_3$ .<sup>21</sup> The appearance of two IR bands at 421 and 381  $\text{cm}^{-1}$ , corresponding to the O–Fe–O deformation vibration, was explained as a deviation from the ideal RE-orthoferrite crystal structure. FT-IR spectrum of sample S10 showed two very broad IR bands positioned at 596–548 and 400  $\text{cm}^{-1}$ . In line with XRD analysis it can be concluded that the Pr–O and O–Pr–O vibrations of  $\text{Pr}_6\text{O}_{11}$  and  $\text{PrO}_2$  predominantly contribute to this FT-IR spectrum.

Figure 3. shows FE-SEM images of selected samples S1 and S8. The image of sample S1 shows micron and submicron hematite particles (Figure 3a.). The image of sample S8 also shows similar  $\text{PrFeO}_3$  particles (Figure 3b.). EDS analysis (Figure 4.) of selected area of sample S8 shows the atomic ratio Pr:Fe close to the ratio in  $\text{PrFeO}_3$  in line with the nominal chemical composition shown in Table 1.

## CONCLUSION

Formation of oxide phases in the system Pr–Fe–O at 900 °C was monitored. The molar fraction of  $\text{PrFeO}_3$  increased with increase of the starting molar fraction “ $\text{Pr}_2\text{O}_3$ ”.  $\text{PrFeO}_3$  and small amounts of  $\alpha\text{-Fe}_2\text{O}_3$  and unidentified oxide phase(s) were formed when equal molar fractions of  $\text{Fe}_2\text{O}_3$  and “ $\text{Pr}_2\text{O}_3$ ” were used. With further increase in the molar fraction of “ $\text{Pr}_2\text{O}_3$ ”,  $\text{Pr}_6\text{O}_{11}$  and  $\text{PrO}_2$  started to become dominant in the phase composition. The small fraction ( $< 0.02$ ) of the same unidentified phase was also obtained upon the calcination of pure  $\text{Pr}(\text{OH})_3$  precipitate up to 900 °C. It was suggested that this unidentified oxide phase is very proba-

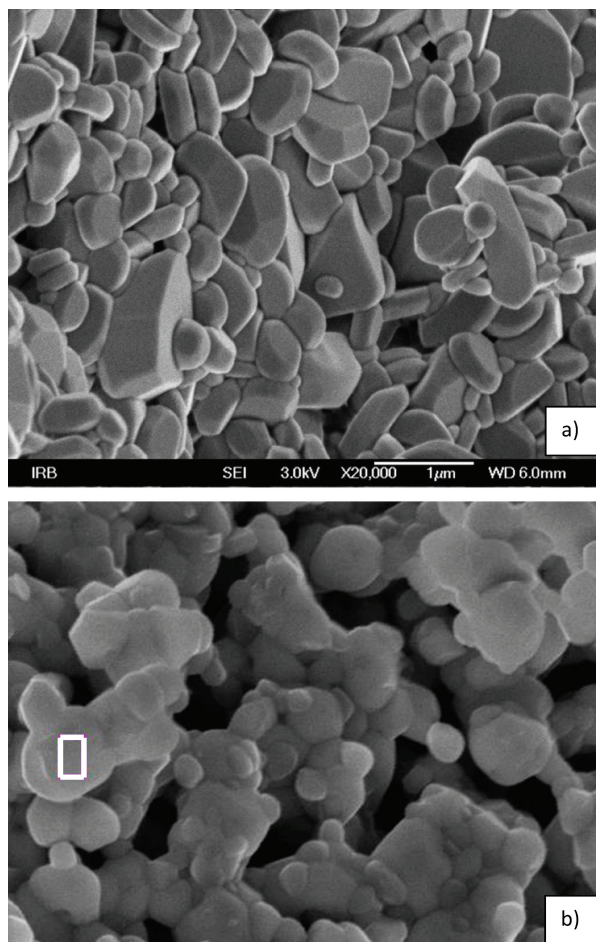


**Figure 3.** FE-SEM images of samples S1 (a) and S8 (b).

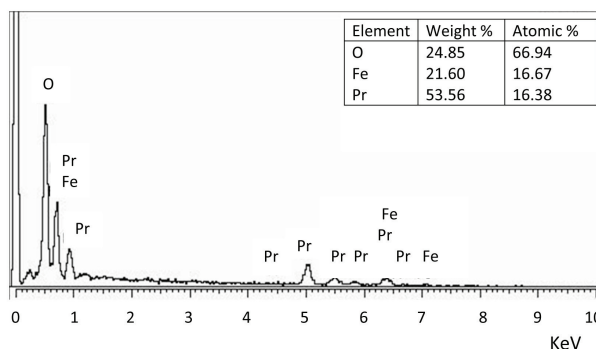


**Figure 4.** EDS spectrum of the particle in sample S8 (selected area in Figure 3b.).

bly a mixture of other praseodymium oxides with different average oxidation numbers of Pr.

## REFERENCES

1. M. Rajendran, M. Ghanashyam Krishna, and A. K. Bhattacharya, *Thin Solids Films* **385** (2001) 230–233.
2. M. Sivakumar, A. Gedanken, D. Bhattacharaya, I. Brukental, Y. Yeshurun, W. Zhong, Y. W. Du, I. Felner, and I. Nowik, *Chem. Mater.* **16** (2004) 3623–3632.

3. M. Rajendran and A. K. Bhattacharya, *J. Eur. Ceram. Soc.* **26** (2006) 3675–3679.
4. L. Zhu, N. Sakai, T. Yanoh, S. Yano, N. Wada, H. Takeuchi, A. Kurokawa, and Y. Ichihyanagi, Proceedings of Asia Pacific Interdisciplinary Research Conference 2011. *J. Physics: Conference Series* **352** (2012) 012021.
5. C. Shivakumara, *Solid State Commun.* **139** (2006) 165–169.
6. X. Li, C. Tang, M. Ai, L. Dong, and Z. Xu, *Chem. Mater.* **22** (2010) 4879–4889.
7. M. A. Ahmed, S. I. El-Dek, *Mater. Sci. Eng. B* **128** (2006) 30–33.
8. M. A. Ahmed, S. I. El-Dek, *Mater. Lett.* **60** (2006) 1437–1446.
9. F. A. Mir, M. Ikram, and R. Kumar, *Philosoph. Magazine* **92** (2012) 1058–1070.
10. I. P. Saraswat, A. C. Vajepi, V. K. Garg, and Nam Prakash, *J. Mater. Sci.* **16** (1981) 433–438.
11. S. Ferro, *Int. J. Electrochem.* **2011** (2011) Article ID 561204.
12. F. J. Lincoln, J. R. Sellar, and B. G. Hyde, *J. Solid State Chem.* **74** (1988) 268–276.
13. Z. C. Kang, L. Eyring, *J. Solid State Chem.* **75** (1988) 52–59.
14. R. Sharma, H. Hinode, and L. Eyring, *J. Solid. State Chem.* **92** (1991) 401–419.
15. L. Eyring, *J. Alloys Comp.* **207/208** (1994) 1–19.
16. E. Murad, J. H. Johnston, *Iron Oxides and Oxyhydroxides*, in G. J. Long (Ed.) *Mössbauer Spectroscopy Applied to Inorganic Chemistry*, Vol. 2, Plenum Publ. Corp., NY, 1987, pp. 507–582.
17. M. Eibschütz, S. Shtrikman, and D. Treves, *Phys. Rev.* **156** (1967) 562–577.
18. M. P. Pasternak, W. M. Xu, G. Kh. Rozenberg, and R. D. Taylor, *Electronic, Magnetic and Structural Properties of the RFeO<sub>3</sub> Antiferromagnetic-Pervoskites at Very High Pressures*, Report LA-UR-02-2720, Edited by Los Alamos National Laboratory, University of California, USA
19. O. Onari, T. Arai, and K. Kudo, *Phys. Rev. B* **16** (1977) 1717–1721.
20. J. L. Rendon, J. Cornejo, P. De Arambarri, and C. J. Serna, *J. Coll. Interface Sci.* **92** (1983) 508–516.
21. W. Zheng, R. Liu, D. Peng, and G. Meng, *Mater. Lett.* **43** (2000) 19–22.